



HAL
open science

Fluvial sand, Amazon mud, and sediment accommodation in the tropical Maroni River estuary: Controls on the transition from estuary to delta and chenier plain

Antoine Gardel, Edward J. Anthony, Valdenira Ferreira dos Santos, Nicolas Huybrechts, Sandric Lesourd, Aldo Sottolichio, Tanguy Maury, Morgane Jolivet

► To cite this version:

Antoine Gardel, Edward J. Anthony, Valdenira Ferreira dos Santos, Nicolas Huybrechts, Sandric Lesourd, et al.. Fluvial sand, Amazon mud, and sediment accommodation in the tropical Maroni River estuary: Controls on the transition from estuary to delta and chenier plain. *Regional Studies in Marine Science*, 2021, 41, pp.101548. 10.1016/j.rsma.2020.101548 . hal-03023544

HAL Id: hal-03023544

<https://hal.science/hal-03023544v1>

Submitted on 25 Nov 2020

HAL is a multi-disciplinary open access archive for the deposit and dissemination of scientific research documents, whether they are published or not. The documents may come from teaching and research institutions in France or abroad, or from public or private research centers.

L'archive ouverte pluridisciplinaire **HAL**, est destinée au dépôt et à la diffusion de documents scientifiques de niveau recherche, publiés ou non, émanant des établissements d'enseignement et de recherche français ou étrangers, des laboratoires publics ou privés.

Journal Pre-proof

Fluvial sand, Amazon mud, and sediment accommodation in the tropical Maroni River estuary: Controls on the transition from estuary to delta and chenier plain

Antoine Gardel, Edward J. Anthony, Valdenira Ferreira dos Santos, Nicolas Huybrechts, Sandric Lesourd, Aldo Sottolichio, Tanguy Maury, Morgane Jolivet



PII: S2352-4855(20)30676-9
DOI: <https://doi.org/10.1016/j.rsma.2020.101548>
Reference: RSMA 101548

To appear in: *Regional Studies in Marine Science*

Received date: 29 April 2020
Revised date: 11 September 2020
Accepted date: 16 November 2020

Please cite this article as: A. Gardel, E.J. Anthony, V.F. dos Santos et al., Fluvial sand, Amazon mud, and sediment accommodation in the tropical Maroni River estuary: Controls on the transition from estuary to delta and chenier plain. *Regional Studies in Marine Science* (2020), doi: <https://doi.org/10.1016/j.rsma.2020.101548>.

This is a PDF file of an article that has undergone enhancements after acceptance, such as the addition of a cover page and metadata, and formatting for readability, but it is not yet the definitive version of record. This version will undergo additional copyediting, typesetting and review before it is published in its final form, but we are providing this version to give early visibility of the article. Please note that, during the production process, errors may be discovered which could affect the content, and all legal disclaimers that apply to the journal pertain.

© 2020 Published by Elsevier B.V.

1 **Fluvial sand, Amazon mud, and sediment accommodation in the tropical Maroni River**
2 **estuary: controls on the transition from estuary to delta and chenier plain**

3 Antoine Gardel¹, Edward J. Anthony^{2,1}, Valdenira Ferreira dos Santos³, Nicolas Huybrechts⁴,
4 Sandric Lesourd⁵, Aldo Sottolichio⁶, Tanguy Maury¹, Morgane Jolivet¹

5 ¹Centre National de la Recherche Scientifique-CNRS, URS3456, 97334 Cayenne, French Guiana.

6 ²Aix Marseille Univ, CNRS, IRD, INRA, Coll France, CEREGE, Aix-en-Provence, France.

7 ³NuPAq, IEPA, Mascara, Brazil.

8 ⁴Cerema, Direction Technique Eau, Mer et Fleuves, 134 rue de Beauvais, 60280 Margny-lès-Compiègne, France.

9 ⁵Université de Caen Basse Normandie, UMR 6143 M2C, Caen, France.

10 ⁶Université de Bordeaux, UMR 5805 EPOC, Bordeaux, France.

11
12 Corresponding author: A. Gardel (antoine.gardel@cnr.fr)

13
14 **Abstract**

15 The Maroni River, South America, is a tropical estuary encased in a narrow lower valley with
16 a limited area of estuarine tidal flat development, and displays a channel with large
17 downstream-migrating sandy bedforms linked to a large sand-filled shallow mouth. The sand-
18 rich nature of the lower Maroni River reflects significant fluvial bedload supply, and the
19 Maroni is among rivers with the lowest suspension-sized sediment load in the world. During
20 the dry season, the estuary shows high suspended sediment concentrations near the bottom
21 (several g/l) that are due to the ingress of mud streaming alongshore from the Amazon River
22 delta. However, Amazon mud is expelled from the estuary during the high-discharge rainy-
23 season, and seems to be essentially restricted to this seasonal intrusion along the main
24 channel with little net estuarine sedimentation because of limited channel overbank sediment
25 accommodation space. Sand actively supplied by the Maroni River to the coast has been
26 diverted by wave-generated longshore transport westwards, towards the Suriname coast.
27 This has resulted in the construction of numerous sandy cheniers within a muddy coastal plain
28 built from Amazon mud. This sediment-source dichotomy is an important original feature of
29 the Guiana Shield estuaries. The asymmetric progradation at the mouth of the Maroni
30 fingerprints the westward growth, in the vicinity of river mouths, of the muddy, chenier-
31 studded, coastal plain of the Guianas. The propensity for these rivers to supply sand to the
32 coast, eventually evolving into deltas, depends on the ability of their estuaries to limit

33 westward (downdrift) deflection by long-term updrift coastal sedimentation. The Maroni
34 estuary has tended to evolve towards a delta built from both Maroni river sand and Amazon
35 mud, a stage, among the Guiana Shield Rivers, that only the large Essequibo River estuary in
36 Guyana has achieved. Further studies will be needed in order to constrain the infill pattern of
37 the Maroni River estuary and its mouth.

38 **Keywords:** tropical estuary; delta; chenier plain; Maroni River; Amazon mud.

39 **Highlight:**

- 40 • Sediment supply and river valley morphology can determine estuary-to-delta transition
- 41 • The narrow tropical Maroni estuary in South America is infilled by fluvial sand
- 42 • High but mobile suspension loads within the estuary are essentially due to Amazon mud
- 43 • Infill of the estuary has been dominated by sand, leading to the emergence of a delta
- 44 • Coastal progradation from Maroni sand and Amazon mud has formed a chenier plain

46 **1. Introduction**

47 River mouths occupy a transitional zone that has been summarised by Dalrymple and Choi
48 (2007) as one that is representative of some of the most profound spatial changes in
49 depositional conditions that can be found anywhere on earth, because of the dramatic
50 variations in many factors that influence the nature of the deposits. This transitional zone is
51 potentially one of significant trapping of both fluvial and marine sediment. Bedload is trapped
52 in the so-called bedload convergence zone, the BLC, whereas fine-grained sediment is
53 commonly concentrated in an estuarine turbidity maximum, the ETM (Dyer, 1997; Uncles,
54 2002; Wolanski, 2007). It is usual to consider that a river supplies both bedload and suspended
55 load, the proportion of the latter tending to increase in tropical rivers with large catchments
56 subject to long-term chemical weathering (Milliman and Meade, 1983), but it is also common
57 to have marine bedload, generally derived from alongshore or from the shoreface, intruding
58 into an estuary (Anthony, 2009).

59 Both the BLC and the ETM illustrate the long-term sediment-trapping capacity of estuaries.
60 Although fine-grained sediment is commonly transported from estuaries onto the coast,

61 especially during high-discharge phases, thus contributing to enhancing turbidity levels
62 alongshore, it is not common to have important fine-grained sediment intrusion into estuaries
63 from the open coast. This can occur, however, in circumstances where large rivers supply
64 massive amounts of mud that are then transported alongshore, sometimes for hundreds of
65 kilometres, in mud dispersal systems driven by wind-, wave and/or tide-induced currents.
66 Such systems can source mud intrusion into smaller rivers located downstream. Lateral mud
67 dispersal is associated with a number of deltaic systems such as the Jaba and Purari in
68 Indonesia (Wright, 1989), the Ayeyarwady, the mud supply of which penetrates into the
69 Sittang River estuary (Shimozono et al., 2019), and the Ganges-Brahmaputra, the mud supply
70 of which maintains the Sundarbans mangroves several hundred kilometres west of the active
71 delta distributary mouths (Bomer et al., 2020). The world's largest and muddiest coast is
72 situated along the Guianas in northern South America between the mouths of the Amazon
73 and the Orinoco Rivers. Mud concentrations exceeding several hundreds of g/l (Gratiot et al.,
74 2007) occur, potentially affecting the numerous smaller Guiana river mouths located between
75 these two big rivers along this 1500 km-long coast. Marine mud sourcing of estuaries can also
76 occur where an alongshore mud belt results from seasonal resuspension of mud on the inner
77 shelf, as along the coast of West Africa between Sierra Leone and Guinea-Bissau (Anthony,
78 2006).

79 Both the BLC and the ETM serve as zones of high sediment concentration but the nature of
80 bedload implies that the BLC is often important to long-term estuarine channel infill, whereas
81 sediment concentrated in the ETM may constitute a much more mobile pool (Uncles, 2002)
82 that may nevertheless be also an important source of fine-grained sedimentation under
83 favourable conditions (Geyer et al., 2004). Sediment from both these features can be
84 transported through the estuary to the open coast, but this can only occur in a sustained way
85 supporting coastal progradation where significant estuarine infilling has occurred, enabling
86 delta growth (Boyd et al., 1992). In addition to sediment supply, the infill transition from
87 estuary to delta is, under conditions of stable sea level, modulated by: (a) the morphological
88 attributes of the lower river valley in which the estuary is encased, the coastal plain and the
89 inner shelf, which determine potential accommodation space for sediments, and (b) the
90 prevailing river, wave and tidal processes which condition sediment concentration, storage
91 and dispersal. A high fluvial sediment supply and small estuarine accommodation space would

92 invariably lead to rapid evolution of estuaries towards deltas where the coastal and shoreface
1 93 morphology and processes are favourable to sediment accumulation. This is a feature
2 94 common in the Mediterranean where there is a plethora of deltas associated with small river
3 95 catchments (Anthony, 2015). The influence of: (1) bedload supply, (2) mud supply, and (3)
4 96 accommodation space in determining aspects of estuarine development and evolution
5 97 towards the delta stage are examined for the Maroni River in South America (Fig. 1a). The
6 98 Maroni is, as shown below, a tropical river particularly rich in bedload supply potentially
7 99 favourable to coastal progradation, but one also having a narrow estuary potentially subject
8 100 to the ingress of mud in transit alongshore from the mouths of the Amazon located
9 101 approximately 750 km to the southeast. This combination of fluvial bedload supply and mud
10 102 from the Amazon expresses a major original feature regarding the sedimentary dynamics and
11 103 geomorphic development of this tropical estuary. The present study examines the way these
12 104 two sediment sources have, together with the inherited estuarine morphology, played out in
13 105 the long-term morphological development of the Maroni river mouth.
14
15
16
17
18
19
20
21
22
23
24
25
26
27
28
29
30

107 2. Study area and methods

108 2.1. Maroni River and estuary

109 The Maroni River (Fig. 1) is 612-km long and has a catchment area of 66,184 km², making
110 it one of the larger of the numerous 'small' rivers of the Guiana Shield between the mouths
111 of the Amazon (catchment size: 3.6 million km²), and the Orinoco (catchment size: 1.1 million
112 km²). The Maroni catchment experiences a humid tropical-equatorial seasonal climate
113 modulated by the north-south movement of the Intertropical Convergence Zone (ITZC). The
114 rainy season lasts from the end of December to July and the dry season from August to
115 December. The rainy season is usually interrupted by a 1-month 'little' dry season in March.
116 Rains are generated by onshore-directed northeast trade winds, whereas offshore southwest
117 trade winds are dominant when the ITZC moves offshore of the South American coast during
118 the dry season. The Maroni has a mean water discharge of ~1700 m³/s, with a range from
119 ~774 m³/s during the dry season to ~2400 m³/s during the rainy season, when the maximum
120 can exceed ~3500 m³/s (Rousseau et al., 2019; Abascal et al., 2020). The mean discharge is
121 over 100 times less than that of the Amazon. Rousseau et al. (2019) showed that the Maroni's
122

122 seasonality index, defined as the ratio between the highest and lowest monthly discharge, is
123 much higher than that of the Amazon, thus highlighting the strongly seasonal character of the
124 river's water discharge as well as a catchment-dampening and flow-smoothing capacity on
125 water discharge that are much smaller than those of the much larger Amazon. The Maroni has
126 been identified as among the world's rivers with the lowest suspended sediment
127 concentrations (Sondag et al., 2010), a characteristic shared by other Guiana Shield rivers
128 (Oliveira and Clavier, 2000). This reflects, no doubt, the highly crystalline basement rocks but
129 also the still largely forested nature of the catchments. Rousseau et al. (2019) found marked
130 differences in the geochemical composition (Al/Si ratios, weathering indices, $^{87}\text{Sr}/^{86}\text{Sr}$) of
131 suspended particulate matter (SPM) in the Amazon, Orinoco and Maroni Rivers, and noted
132 that the Sr isotopic composition of SPM appears to be mostly controlled by weathering
133 processes and/or mineralogical sorting, rather than being indicative of sediment provenance.
134 A >200% increase in SPM in the Maroni since 2009 has been reported by Gallay et al. (2018)
135 who attributed this to anthropogenic activities, notably gold mining and deforestation. The
136 Maroni River forms much of the frontier between French Guiana and Suriname and its banks
137 host the twin towns of St. Laurent du Maroni (French Guiana) and Albina (Suriname) about 30
138 km upstream from the estuary mouth. These are among the fastest growing towns in the
139 Guianas, notably St. Laurent du Maroni, where port facilities capable of handling large ocean-
140 going vessels are being planned, providing a further justification for a better understanding of
141 the functioning of the Maroni's estuarine system. Following an early preliminary study on the
142 suspended sediment regime of the river (Jouanneau and Pujos, 1988), the lower Maroni and
143 its estuary have attracted attention in a number of recent studies that have focused on field
144 monitoring of bedforms at the mouth (Bureau de Recherches Géologiques et Minières, 2017,
145 2019), the estuarine tidal structure and flows (Sottolichio et al., 2018; Ross et al., 2019),
146 modelling of the tidal circulation (Do et al., 2019), and remote-sensing and field-based
147 analyses of recent shoreline geomorphic changes at the estuary mouth (Jolivet et al., 2019a,
148 2019b), and the dynamics of the estuarine turbidity maximum (Abascal et al., 2020).

149 Tides in the Maroni estuary are mesotidal and semidiurnal, with a range of up to 2.5 m
150 during spring tides at kilometric point (KP) 0 (Fig. 1b), and a slight amplification to a maximum
151 of 2.65 m at about KP 15 (Sottolichio et al., 2018). Two large tidal creeks, the Coswine and the
152 Vaches, debouch on the east bank of the estuary near the mouth, and a series of shoals and

153 vegetated islands have accumulated between KP 15 and KP 26.5 (Fig. 1). Waves in the Maroni
154 estuary area arrive from an east to northeast direction in response to the predominant trade
155 winds (Gratiot et al., 2007). Waves with significant heights exceeding 2 m prevail between
156 October and May, while waves are lower (significant wave heights <1 m) from June to
157 September. Waves undergo important dissipation over an east-west migrating mud bank that
158 has been encroaching on the estuary since 2011, as well as over the large shallow sand banks
159 at the mouth of the estuary (Jolivet et al., 2019a).

160 2.2. Methods

161 The morphology of the Maroni estuary and the adjacent coasts of French Guiana and
162 Suriname has been characterized from Landsat and Sentinel 2A satellite images and aerial
163 photographs, thus, providing a template for identification of multi-decadal patterns of
164 sediment redistribution, extent of the estuarine plain, and the ensuing coastal accretion.
165 Shoreline changes in the vicinity of the estuary mouth have been reported by Anthony et al.
166 (2019a) and Jolivet et al. (2019a, 2019b), respectively, for the Suriname and French Guiana
167 sectors.

168 In order to characterize the subtidal morphology of the estuary, two complementary
169 bathymetric surveys were conducted in October 2016 and in May 2017 using a Valeport Midas
170 echosounder with a dual-frequency (33–210 kHz) single beam and integrated DGPS. The DGPS
171 precision is ± 2 m and that of the echosounder 0.01 m. The October 2016 survey concerned
172 the estuarine reach from the mouth to Saint Laurent du Maroni (Fig. 1b), and was conducted
173 using a cross-channel transect spacing of 350 m, yielding a total of 70 transects. The data was
174 treated to generate a digital elevation model (DEM) with 10 m-cells. Water level fluctuations
175 due to tides were corrected using records from three pressure sensors evenly spaced along
176 the 30-km channel axis. Observations of intertidal bedforms on the large estuarine sand
177 platform and adjacent beaches were also conducted in the course of this survey. The May
178 2017 survey covered the large sandy platform in the estuary mouth and the shoreface (Fig.
179 1b). In the course of this survey, hydromagic software was used for synchronization of the
180 data with the recorded positions from the DGPS. The survey was conducted along 8 transects
181 spaced 2 km, and 200-m DEM cells were generated.

182 Measurements of salinity and suspended sediment concentrations (SSC) were conducted
183 in the course of several seasons in the water column from the surface to the channel bottom
184 between KP 0 and KP 30 (Fig. 1b). The measurements reported here are part of an on-going
185 series of surveys (see Do et al., this issue, for details). Here, we focus on the situation observed
186 on 29th September, 2019, in the course of a semi-diurnal spring tidal cycle during the dry
187 season. The measurements were made every 1 km at high tide during slack water along a
188 profile in the channel using the moving vessel method (Savenije 1989). Salinity was measured
189 using a conductivity-temperature-depth probe (CTD CastAway © SonTek), and turbidity using
190 a turbidity probe (OBS 5+ © Campbell Scientific). The turbidity signal was converted into SSC
191 using a calibration curve built in the laboratory.

193 3. Results

194 The Maroni exhibits a relatively narrow estuarine valley and a wide mouth displaying an
195 asymmetric pattern of coastal accretion on either side of the estuarine axis (Fig. 2). The main
196 channel and the narrow estuarine valley are flanked by a coastal plateau comprising
197 Pleistocene deposits and basement rocks (Grua and Cautru, 1993; Augustinus, 2004; Wong et
198 al., 2009), with little in terms of contemporary intertidal estuarine deposits. Coastal accretion
199 at the mouth of the estuary has been more important on the Suriname side than on the French
200 Guiana side, and consists of numerous sandy chenier ridges interspersed in a muddy
201 progradational plain with freshwater marshes. South of Galibi in Suriname, these ridges occur
202 as 'bayside' cheniers (in the terminology of Otvos and Price, 1979) flanking the main estuarine
203 channel and oriented virtually south-north. North of Galibi, the cheniers undergo a change in
204 orientation from south-north to southeast-northwest in phase with the transition from
205 estuary mouth to the open-coast shoreline, and then east-west to follow the current open
206 shoreline trend on this part of the Suriname coast (Fig. 2). Progradation has been less
207 pronounced on the French Guiana bank, although several cheniers are also identified within
208 a muddy coastal plain dominated by freshwater swamps. The earlier ones are also bayhead
209 cheniers, but the coast-parallel cheniers appear to have been constructed from sand supplied
210 by the smaller adjacent Mana River. The mouth of this river was, as suggested by an ancient
211 abandoned trace on aerial photographs, and in agreement with the regional east-west

212 longshore transport on this coast, diverted in the past towards the Maroni estuary (Jolivet et
1 213 al., 2019b). Further south, the east bank of the Maroni is characterized by high stands (up to
2 214 20 m) of *Avicennia germinans* mangroves that give way inland along the tidal Coswine creek
3 215 into shrubby (< 5 m) *Rhizophora racemosa* mangroves up to the contact with the older
4 216 continental deposits where freshwater marshes prevail. Vaches creek is essentially flanked by
5 217 freshwater swamps. The upstream islands near St. Laurent du Maroni are covered by 10-20
6 218 m-tall stands of freshwater forests (Fig. 2).

219 The estuary mouth exhibits a wide, relatively shallow platform (Fig. 3) with large areas
14 219 ranging in depth from 2 to 4 m below French hydrographic datum (0 m). Although much of
15 220 the platform is sandy, a large area in the east is composed of mud much of which is < 1 m
16 221 below 0 datum, highlighting the encroachment of the leading edge of a mud bank, parts of
17 222 which have welded ashore on the French Guiana coast (Fig. 3). The platform is cut by a
18 223 moderately deep (down to -10 m) and relatively straight single channel running north-
19 224 northeast on the French Guiana side, virtually in contact with the open-coast sandy shoreline
20 225 at Yalimapo (Fig. 3). Much of the surface of the platform is covered by hydraulic dunes (Figs.
21 226 4, 5) composed of medium to coarse quartz yellowish sand, fine gravel and broken shells.
22 227 These dunes are medium-sized (0.5 to 2 m), 2D to 3D forms, according to the terminology of
23 228 Ashley (1990). The dunes show a residual migration in the direction of ebb flow, except in the
24 229 main flood-dominated channel, and observations at low tide show that this migration occurs
25 230 over a hard pavement of packed coarse sand and, locally, fine gravel (Jolivet et al., 2019a).

232 Upstream from the mouth, the channel bathymetry shows a complex pattern of shoals
40 232 corresponding to elongate sand banks alternating with deeper areas with fluid mud. The sand
41 233 here is reddish compared to the yellow sand of the estuarine platform, thus probably
42 234 indicating progressive downstream loss of the ferruginous coating associated with fresh inputs
43 235 from the catchment. Depths are up to 20 m in some areas, even close to the river banks and
44 236 preliminary on-going bed sampling (not reported here) shows that these areas comprise
45 237 weathered bedrock and laterite. Shallow areas occur in the vicinity of Vaches creek and
46 238 downstream of Saint Laurent du Maroni where sand banks line the river bank, but even in
47 239 these creeks, there are areas where the channel bottom consists of bedrock. Boomer seismic
48 240 observations (Bureau de Recherches Géologiques et Minières, 2017, 2019) show that the main
49 241 estuarine channel is rich in sand waves with steep stoss slopes oriented downstream.
50 242

243 The salinity intrusion length in the Maroni varies seasonally, reaching ~27 km upstream
1 from the mouth during dry season (Fig. 6a) but only ~5 km during the rainy season (Do et al.,
2 244 this issue). The dry season measurements carried out on 29th September 2019 show a clear
3
4 245 stratification marked by a salty mass of water at the bottom (salinity values up to 33) in the
5
6 246 downstream part of the estuary up to about KP 6 (Fig. 6a). The water mass then becomes
7
8 247 more mixed, with salinity decreasing progressively up to KP 27. There is little vertical change
9
10 248 in salt values from KP 6 to KP 33 (Fig. 6a), and this corroborates the dry-season observations
11
12 249 of Sottolichio et al. (2018). These authors also highlighted a high degree of seasonality in the
13
14 250 estuary's turbidity and identified an ETM during the rainy season at the mouth.
15
16 251

18 252 The SSC values show a clearly vertical structure with a diminishing trend towards the top
19
20 253 of the water column (Fig. 6b). High SSC of 2.5 to about 4 kg/m³ form layers 1-2.5 m-thick over
21
22 254 variable channel-bed topography, and up to KP 27 km upstream the mouth (Fig. 6b).
23
24
25 255

28 256 4. Discussion

30 257 Between the mega river-mouths of the Amazon and the Orinoco are numerous smaller
31
32 258 rivers debouching onto the Atlantic Ocean, such as the Maroni, and the estuaries of which lie,
33
34 259 thus, along the coastal migration pathway of mud banks from the Amazon. One long-term
35
36 260 effect of Amazon mud has been deflection of the mouths of many of these estuaries by large-
37
38 261 scale sedimentation in the form of mud capes (Augustinus, 1978, 2004; Anthony et al., 2010;
39
40 262 Jolivet et al., 2019b). These mud capes are systematically oriented northwestward or
41
42 263 westward (depending on the regional coastal trend), reflecting the influence of the
43
44 264 northeasterly trade-wind waves that are the main driver of mud-bank migration and long-
45
46 265 term muddy sedimentation along the Guianas coast (Gratiot et al., 2007). Another important
47
48 266 effect is that as the banks impinge on these smaller estuaries, they serve as an important
49
50 267 external source of mud that is transported upstream by tidal currents (Orseau et al., 2017,
51
52 268 2020; Abascal et al., 2020). The extraneous mud supply, thus, has implications not only for the
53
54 269 short-term estuarine dynamics but also for the longer-term estuarine morpho-sedimentary
55
56 270 development. These smaller rivers drain the crystalline basement rocks of the Guiana Shield,
57
58 271 and are, thus, potentially important purveyors of sand that can eventually be supplied to the
59
60 272 coast to build cheniers in this predominantly muddy setting (Anthony et al., 2019a). The
61
62
63
64
65

273 propensity for these rivers to supply sand to the coast, eventually evolving into deltas,
1 274 depends, however, on the ability of their estuaries to limit westward (downdrift) deflection
2 275 by long-term updrift coastal sedimentation.
3
4
5

6 276 To conceptually gauge the long-term capacity of river mouths in countering the alongshore
7 277 deflective effect of mud from the Amazon on the morphological plan shape of Guiana Shield
8 278 estuaries, Anthony et al. (2013) identified two basic types of estuaries. The first is
9 279 characteristic of the small-catchment rivers (catchment size $< 20,000 \text{ km}^2$) and the discharge
10 280 of which is too low to counter the alongshore deflective effect. The second type concerns the
11 281 larger rivers (catchment size $> 20,000 \text{ km}^2$) characterized by water discharge and tidal
12 282 pumping strong enough to keep the estuary non-deflected and open, although mud may
13 283 accumulate on either side, and commonly significantly intrudes up-estuary, as discussed
14 284 below. The authors assimilated this counter-deflection to a 'hydraulic-groyne' effect (Todd,
15 285 1968) that may favour accretion on the updrift coast without the emergence of a mud cape.
16 286 The Maroni is a fine example of this estuarine type (Fig. 1b). Its mouth shows a stationary non-
17 287 deflected position relative to the rectilinear axis of the estuarine channel. Notwithstanding
18 288 this, however, the Maroni River estuary occupies a complex coastal setting where an
19 289 important accumulation of fluvial bedload has co-existed with extraneous mud from the
20 290 Amazon. The long-term estuarine infill and coastal accretion reflect this specificity, which is
21 291 expressed by spatial variations in sedimentology and geomorphology (Fig. 2).
22
23
24
25
26
27
28
29
30
31
32
33
34
35
36
37

38 292 The dry-season salinity and SSC structure in the axis of the Maroni estuary shows the
39 293 pervasive influence that mud supply associated with migrating mud banks appears to have in
40 294 the seasonal estuarine dynamics. The large dry-season SSC values reported here following the
41 295 brief experiment in 2019 (Fig. 6b) do not appear to correspond to a classic ETM associated
42 296 with the freshwater-salt water convergence. However, longer time series of measurements
43 297 led Do et al. (this issue) to identify a dry-season ETM that they attribute to possible
44 298 resuspension by tidal currents and convergence of gravity circulation, a point also raised by
45 299 Abascal et al. (2020). Do et al. (2019) and Do et al. (this issue) show, indeed, strong seasonal
46 300 contrasts in suspended solid concentrations, with a very turbid estuary in the dry season and
47 301 clearer waters in the rainy season. They also highlighted the persistence of an ETM near the
48 302 mouth in the course of the latter season. The authors identified the dry-season ETM location
49 303 upstream, in the vegetated island sector. Both Do et al. (2019) and Ross et al. (2019) also
50
51
52
53
54
55
56
57
58
59
60
61
62
63
64
65

304 showed from velocity measurements that the Maroni is largely characterized by residual ebb-
1 305 dominated flow, especially when rainy season discharge enhances outflow.
2
3

4 306 The high dry-season SSC values in Fig. 6b are not likely to represent mud derived from
5
6 307 fluvial sediment discharge, given the and low river flow and low SSC from the Maroni
7
8 308 catchment, even when the recent anthropogenically-induced increase in fine-grained
9
10 309 sediment supply (Gallay et al., 2018) is taken into account. We deduce that intrusive mud is:
11
12 310 (1) derived from the nearby high-concentration mud pool represented by the mud bank that
13
14 311 has been migrating across the Maroni mouth since 2011 (Fig. 2), and (2) transported
15
16 312 essentially through the eastern channel that links up with the main estuarine axis. Ross et al.
17
18 313 (2019) identified this channel on the French Guiana side as flood-dominated. This mud is
19
20 314 trapped near the bed (Fig. 6b), consistent with the upstream salt intrusion (Fig. 6a) which
21
22 315 probably drives this SSC structure. Trapping appears to be dynamic, rather than topographic,
23
24 316 as the dense mud lenses are not necessarily found in pools within the channel. They are, thus,
25
26 317 probably mobile. Abascal et al. (2020) have reported from detailed analysis of OLI Landsat
27
28 318 images that the ETM developed in the Maroni estuary during the rainy season is significantly
29
30 319 sourced by Amazon mud, an observation consistent with those of Orseau et al. (2017) on
31
32 320 another estuary in eastern French Guiana, and Asp et al. (2018) on an estuary in Brazil affected
33
34 321 by Amazon mud. All of these observations highlight the complementarity between the
35
36 322 geomorphic approach adopted here and both physical modelling (Do et al., this issue) and
37
38 323 remote sensing approaches (Abascal et al., 2020) in gaining a better understanding of the
39
40 324 dynamics and evolution of estuaries.
41

42 325 The muddy deposits associated with the small areas of tidal flats on the French Guiana side,
43
44 326 and the vegetated islands near St. Laurent du Maroni (Fig. 2) likely reflect input from Amazon
45
46 327 mud in their long-term sedimentation. This is expected, given not only the importance of
47
48 328 Amazon mud intrusion but also the extremely low values of terrigenous suspended loads
49
50 329 brought downstream by the river. This fluvial suspension load mixes with mud from the
51
52 330 Amazon (Jouanneau and Pujos, 1988). As a consequence, the expected geochemical signature
53
54 331 of the estuarine SSC will not display differences between the Maroni and the Amazon noted
55
56 332 by Rousseau et al. (2019), who sampled the Maroni at the hydrological station of Langa Takaki
57
58 333 about 80 km upstream of the mouth, well above the estuarine zone. Estuarine sedimentation
59
60 334 sourced by Amazon mud has been rather limited from a surface area perspective, given the
61
62
63
64
65

335 narrow nature of the Maroni valley, but its vertical extent, dependent on the depth of valley
1
2 336 incision during the last sea-level lowstand, is not known. Potentially, the ETM, involving
3
4 337 Amazon mud and a low river-derived contribution, and shown to expand during the present
5
6 338 phase of mud bank intrusion on the Maroni (Abascal et al., 2020), has acted as a seasonally
7
8 339 mobile mud pool. From this pool, sediment, mobilized by high discharge in the rainy season
9
10 340 and by tidal pumping, especially during spring tides, is deposited to build up the small areas
11
12 341 of peripheral tidal flats, as well as the island sector. Do et al. (this issue) identify a strong rainy-
13
14 342 season flushing effect on the ETM resulting from the significantly higher Maroni water
15
16 343 discharge, this leading to clearer waters in the estuary during this season. Potentially,
17
18 344 therefore, although suspended sediment can reach high concentrations in the Maroni estuary,
19
20 345 the dynamics are probably dominated by up-estuary (dry season) and down-estuary (rainy
21
22 346 season) movement of the mobile high SSC pool, with limited peripheral accumulation in
23
24 347 intertidal areas. The limited area of tidal flat development in the estuary reflects, in itself,
25
26 348 inherited antecedent geomorphic control at the end of the post-glacial marine transgression
27
28 349 c. 5-6000 years ago when a relatively narrow Maroni valley was invaded by the sea to form
29
30 350 the current estuary, initiating infill. The morphology and sedimentology of the bed of the
31
32 351 estuary and the large estuary mouth show the overarching dominance of sand in the estuarine
33
34 352 infill and peripheral coastal accretion, with a clear asymmetry between the Suriname and the
35
36 353 French Guiana sides.

37
38 354 The lower valley and estuary have, thus, been largely infilled with sand supplied by the
39
40 355 river, although Jolivet et al. (2019a) also speculated that the large estuary-mouth sand
41
42 356 platform may also have received sand from the adjacent Mana River in the east. The Mana is
43
44 357 a small (catchment size: 12,090 km²; mean discharge: 320 m³/s) type 1 river the mouth of
45
46 358 which was diverted westward by a large 10 km-long mud cape since at least the mid-19th
47
48 359 century (Plaziat and Augustinus, 2004) to join up with the Maroni near Yalimapo. Massive
49
50 360 erosion and demise of the cape have occurred over the last 60 years, resulting, in 2011, in the
51
52 361 relocation of the mouth of this river several kilometres eastward of its former historical mouth
53
54 362 near that of the Maroni (Jolivet et al. (2019b). The large sand platform at the mouth of the
55
56 363 Maroni does not correspond to the classic river-mouth BLC wherein sand converges from both
57
58 364 the river and the shoreface, as classically observed in estuaries, and which is important in
59
60 365 driving estuarine infill (Dyer, 1997; Uncles, 2002; Dalrymple and Choi, 2007). The Maroni sand
61
62
63
64
65

366 platform occupies a zone of convergence of fluvial outflow and tidal intrusion that also lies in
1 367 the regional Amazon mud-bank migration pathway. Jouanneau and Pujos (1988) suggested
2 368 that sand supply from the Maroni on the platform may have been greater during the periods
3
4 369 of lower sea level during the Quaternary. However, the lack of bedload supply from the
5
6 370 shoreface, due largely to blanketing of relict shoreface sand by this pervasive mud supply from
7
8 371 the Amazon (Anthony et al., 2002), has implied that the BLC is virtually exclusively composed
9
10 372 of bedload supplied by this Guiana Shield river, the catchment of which is composed of rocks
11
12 373 that liberate quartz and ferruginous sand and gravel. Sand accumulation at the mouth of the
13
14 374 estuary may also have been enhanced by viscous energy dissipation of tidal and river outflow
15
16 375 involved in the liquefaction of mud banks as they slowly migrate across the mouth of the
17
18 376 Maroni. The significant downstream accumulation of fluvial sand also reflects the present
19
20 377 dominance of downstream-directed residual currents in the estuary highlighted by Do et al.
21
22 378 (2019) and Ross et al. (2019). The latter authors identified a shallow ebb channel at the west
23
24 379 bank of the estuary (Suriname) in addition to the flood-dominated channel on the French
25
26 380 Guiana side. Upstream from the infilled mouth, the elongated sandy shoals and banks that
27
28 381 have accumulated in the Maroni estuarine channel testify to the progressive downdrift
29
30 382 migration of fluvial sand. These deposits will have to be dredged in the future to allow access
31
32 383 to container ships in the developing port of Saint Laurent du Maroni.
33
34

35 384 Coastal accretion sourced by sand from the Maroni and mud from the Amazon has been
36
37 385 more limited on the French Guiana side, as attested by optically stimulated luminescence ages
38
39 386 >2000 years B.P. about 200 m behind the present beach at Yalimapo (Brunier et al., 2019).
40
41 387 Multi-decadal scale shoreline mobility on this side of the river mouth has been shown to be
42
43 388 relatively weak, largely within error margins (a few metres) of analysis, although more marked
44
45 389 mobility occurs where the estuarine flood channel lies close to the beach at Yalimapo (Jolivet
46
47 390 et al., 2019a). The asymmetric accretion pattern of the Maroni on either side of its mouth
48
49 391 clearly shows, thus, that part of the bedload supplied by the river has been incorporated into
50
51 392 the numerous bundles of cheniers that line the Suriname coast, first as bayhead cheniers at a
52
53 393 time when refraction and dissipation of waves from the northeast across the estuary mouth
54
55 394 were much less than at present due to less sandy infill. The changes in the orientation of these
56
57 395 cheniers to a more open-coast east-west alignment have gone apace with the northward
58
59 396 asymmetric progradation of the Suriname side (Fig. 7). The cheniers are incorporated in a
60
61
62
63
64
65

397 muddy plain built from Amazon mud. Sand stored by the large estuarine sand platform has
1 398 been redistributed along the Suriname coast as cheniers as far west (nearly 150 km) as the
2 399 approaches to the next estuary on this coast, the Suriname River estuary (Anthony et al.,
3 400 2019a). Multi-decadal shoreline mobility on this Suriname side has been shown to fluctuate
4 401 largely with episodes of welding of mud from passing mud banks when rapid accretion of up
5 402 to 100 m can occur, followed by nearly proportionately important erosion of mud attended
6 403 by shoreline reworking and concentration of sand to form cheniers (Anthony et al., 2019a).
7 404 The long-term infill pattern and chronological frame of the accretion dynamic on this coast,
8 405 involving chenier ridges and muddy progradation from Amazon mud, still need to be
9 406 determined. The present Maroni river-mouth setting and morphology involve a complex series
10 407 of primary mud and sand transport processes and pathways, as well as more local sand
11 408 pathways that are conceptually summarized in Fig. 8. These pathways result from a
12 409 combination of large-scale drivers, such as river outflow, tidal pumping within the axis of the
13 410 estuary, wave modification and wave-generated longshore transport downdrift of the mouth
14 411 on the Suriname coast, and morphological feedback effects such as mud-bank migration and
15 412 mud intrusion into the Maroni estuary. But there are also more local effects at play, such as
16 413 sand transport rotation involving counter-drift along the beach adjacent to the estuary on the
17 414 French Guiana side (Jolivet et al., 2019a).

35 415 Notwithstanding an asymmetric pattern of accretion, the mouth of the Maroni has
36 416 significantly prograded, generating a morphology akin to that of a delta, rather than an
37 417 estuary. This pattern of coastal development in the vicinity of a river mouth involving muddy
38 418 growth with interspersed cheniers is a common feature of many deltas associated with an
39 419 adequate supply of bedload-sized sediment in a context of ambient mud abundance, as in the
40 420 cases of the deltas of the Huanghe (e.g., Saito et al., 2000), the Changjiang delta (Hori et al.,
41 421 2001), and the Mississippi (McBride et al., 2007). However, in some deltas such as the Red
42 422 River (van Maren, 2005), the Mekong (Tamura et al., 2012), and the Ayeyarwady (Anthony et
43 423 al., 2019b), sandy deposits form discrete barriers separated from each other by tributary
44 424 mouths. These barriers develop from mouth-bars that progressively aggrade under the
45 425 influence of waves, and notably swash processes, to finally isolate back-barrier spaces that
46 426 are eventually filled by mud, giving a superficial impression of chenier-plain development.

427 Intermediate stages such as those shown by the Maroni are also associated with estuaries
1 428 (e.g., Anthony, 1989, 2006; Hein et al., 2016).
2
3

4 429 It is possible to further distinguish, among the type 2 estuaries identified by Anthony et al.
5
6 430 (2013) on plan-view morphological grounds, between those close to a delta morphology and
7
8 431 those that are still far from this morphology. Among the former, the only one that appears to
9
10 432 fit into this category with the Maroni is the Essequibo River (catchment size: 154,860 km²) in
11
12 433 Guyana (Fig. 9a). Although several other estuaries are characterized by a relatively 'rectilinear'
13
14 434 main channel axis with no diversion by a mud cape formed from Amazon mud, they are
15
16 435 estuaries still largely subject to infilling, a fine example being the Coppename River (catchment
17
18 436 size: 54,000 km²) estuary at the border between Suriname and Guyana (Fig. 9b). These
19
20 437 estuaries are still far from the delta stage, while a few estuaries pertaining to the 'small' type
21
22 438 1 category have fairly rectilinear estuaries with mouths fixed by bedrock (Gardel et al., 2019).
23
24 439 In being a significant purveyor of fluvial sand for open-coast chenier development in
25
26 440 Suriname, without having received marine sand as is commonly the case of many infilling
27
28 441 estuaries, the Maroni has progressively acquired the makings of a delta. It has developed from
29
30 442 a deep open estuary with bayside cheniers to a strongly infilled ebb-dominated estuary and a
31
32 443 deltaic purveyor of sand for coastal progradation (Fig. 7). Morphologically, the dominant
33
34 444 influence of the river, aided by strong tidal pumping, is clearly manifest in the open and non-
35
36 445 diverted nature of the large mouth, reflecting clear mitigation of wave influence (Anthony,
37
38 446 2015), and by the pervasive ebb-dominated orientation of the dunes on the estuarine sand
39
40 447 platform. Within this overall deltaic development, advection of Maroni sand towards
41
42 448 Suriname has been the overarching driver of river-mouth and coastal accretion. This
43
44 449 corresponds to the dominant longshore transport direction on the Guianas coast downdrift of
45
46 450 the wave-dissipating Maroni estuarine sand platform where open-coast wave influence in
47
48 451 Suriname becomes strong once more. The ebb-dominated channel identified by Ross et al.
49
50 452 (2019) on the Suriname side is clearly consistent with estuarine infill and with this sand export
51
52 453 pathway, whereas ingress of the Amazon mud, which we deem to be largely mobile up and
53
54 454 down the estuary, without dominating long-term estuarine infill, occurs through the flood-
55
56 455 dominated channel in the east, also identified by these authors. As infill has proceeded, wave
57
58 456 influence has diminished, reflected by the change from bayside cheniers to open-coast
59
60 457 cheniers. This wave influence is now limited to the peripheral beaches, and especially the
61
62
63
64
65

458 Suriname chenier coast downdrift of the mouth. This wave influence has always been
1
2 459 periodically mitigated by the dissipative effect of passing mud banks since the inception of the
3
4 460 Maroni River estuary.

5
6 461

9 462 **5. Conclusions**

10
11
12 463 1. The Maroni River exhibits an estuary encased in a narrow lower river valley with a limited
13
14 464 area of estuarine tidal flat development, while displaying a large sand-filled shallow mouth.
15
16 465 The estuary lies in the pathway of mud banks migrating alongshore from the mouths of the
17
18 466 Amazon to those of the Orinoco.

19
20
21 467 2. The sand-rich nature of the lower Maroni River reflects significant fluvial bedload supply
22
23 468 from the crystalline catchment rocks, while Amazon mud seems to be essentially restricted to
24
25 469 seasonal dry-season intrusion in the estuary and rainy-season expulsion with little net
26
27 470 sedimentation because of limited overbank estuarine sediment accommodation space.

28
29
30 471 3. The geomorphic observations reported here show complementarity with both physical
31
32 472 modelling (Do et al., submitted, this issue) and remote sensing approaches (Abascal et al.,
33
34 473 2020) in gaining a better understanding of the dynamics and evolution of estuaries.

35
36 474 4. Advanced infill of the Maroni River estuary and active fluvial sand supply to the coast have
37
38 475 led to the emergence of a delta marked by the construction, in Suriname, of numerous sandy
39
40 476 cheniers within a muddy coastal plain built from mud supplied by the Amazon. This pattern of
41
42 477 geomorphic development, from an estuary to a delta incorporating cheniers, is typical of many
43
44 478 river deltas elsewhere.

45
46
47 479 5. The infill pattern of the Maroni River estuary, its evolution towards a delta, the associated
48
49 480 asymmetric coastal progradation, and the geochronological frame of these events, will require
50
51 481 further studies.

52
53 482

56 483 **Acknowledgements**

484 Financial support for this work was provided by the European Regional Development Fund
1 485 through the project OYAMAR. Additional support was provided within the framework of the
2 486 project MORPHOMAR funded through the “Pépinière Interdisciplinaire de Guyane” by the
3 487 Centre National de Recherche Scientifique (CNRS), and the Bureau de Recherches
4 488 Géologiques et Minières (BRGM). This is a contribution of the French GDR LIGA researcher
5 489 network. We acknowledge the salient suggestions for improvement from two anonymous
6 490 reviewers.
7
8
9

10 491

13 492 **References**

- 16 493 Abascal Zorrilla, N., Vantrepotte, V., Ngoc, D.D., Huybrechts, N., Anthony, E.J., Gardel, A.,
17 494 2020. Dynamics of the estuarine turbidity maximum zone from Landsat-8 data: the case
18 495 of the Maroni River estuary, French Guiana. *Remote Sensing*, 12, 2173;
19 496 doi:10.3390/rs12132173
- 22 497 Anthony, E.J., 1989. Chenier plain development in northern Sierra Leone, West Africa.
23 498 *Marine Geology*, 90, 297-309. [https://doi.org/10.1016/0025-3227\(89\)90132-1](https://doi.org/10.1016/0025-3227(89)90132-1)
- 24 499 Anthony, E.J., 2006. The muddy tropical coast of West Africa from Sierra Leone to Guinea-
25 500 Bissau: geological heritage, geomorphology and sediment dynamics. *Africa Geoscience*
26 501 *Review*, 13, 227-237.
- 28 502 Anthony, E.J., 2009. Shore Processes and their Palaeoenvironmental Applications.
29 503 *Developments in Marine Geology*, Volume 4. Elsevier Science, Amsterdam, 519 pp.
- 31 504 Anthony, E.J., 2015. Wave influence in the construction, shaping and destruction of river
32 505 deltas: A review. *Marine Geology*, 361, 53-78.
33 506 <https://doi.org/10.1016/j.margeo.2014.12.004>
- 35 507 Anthony, E.J., Besset, M., Dussouillez, P., Goichot, M., Loisel, H., 2019b. Overview of the
36 508 Monsoon-influenced Ayeyarwady River delta, and delta shoreline mobility in response to
37 509 changing fluvial sediment supply. *Marine Geology*, 417, 106038.
38 510 <https://doi.org/10.1016/j.margeo.2019.106038>
- 40 511 Anthony, E.J., Brunier, G., Gardel, A., Hiwat, M., 2019a. Chenier morphodynamics and degradation on the Amazon-influenced
41 512 coast of Suriname, South America: implications for beach ecosystem services. *Frontiers in*
42 513 *Earth Science*, 7, 35, doi: 10.3389/feart.2019.00035
- 44 514 Anthony, E. J., Gardel, A., Proisy, C., Fromard, F., Gensac, E., Péron., C., Walcker, R., Lesourd,
45 515 S., 2013. The role of fluvial sediment supply and river-mouth hydrology in the dynamics of
46 516 the muddy, Amazon-dominated Amapá-Guianas coast, South America: a 3-point research
47 517 agenda. *Journal of South American Earth Sciences*, 44, 18-24.
48 518 <https://doi.org/10.1016/j.jsames.2012.06.005>
- 50 519 Anthony, E.J., Gardel, A., Gratiot, N., Proisy, C., Allison, M.A., Dolique, F., Fromard, F., 2010.
51 520 The Amazon-influenced muddy coast of South America: A review of mud-bank-shoreline
52 521 interactions. *Earth-Science Rev.* 103, 99–121.
53 522 <https://doi.org/10.1016/j.earscirev.2010.09.008>
- 55 523 Anthony, E.J., Gardel, A., Dolique, F., Guiral, D., 2002. Short-term changes in the plan shape of
56 524 a sandy beach in response to sheltering by a nearshore mud bank, Cayenne, French Guiana.
57 525 *Earth Surface Processes and Landforms*, 27, 857-866.
58 526 <http://onlinelibrary.wiley.com/doi/10.1002/esp.357/full>

- 527 Ashley, G. M., 1990. Classification of large-scale subaqueous bedforms; a new look at an old
1 528 problem. *J. Sediment. Res.* 60, 160–172. <https://doi.org/10.2110/jsr.60.160>
- 2 529 Asp, N.E., Gomes, V.J.C., Schettini, C.A.F., Souza-Filho, P.W.M., Siegle, E., Ogston, A.S.,
3 530 Nittrouer, C.A., Silva, J.N.S., Nascimento, W.R., Souza, S.R., Pereira, L.C.C., Queiroz, M.C.,
4 531 2018. Sediment dynamics of a tropical tide-dominated estuary: Turbidity maximum,
5 532 mangroves and the role of the Amazon River sediment load. *Estuar. Coast. Shelf Sci.* 214,
6 533 10–24. <https://doi.org/10.1016/j.ecss.2018.09.004>
- 7 534 Augustinus, P.G.E.F. 1978. The changing shoreline of Surinam (South America). Ph.D. thesis,
8 535 University of Utrecht.
- 9 536 Augustinus, P.G.E.F. 2004. The influence of the trade winds on the coastal development of the
10 537 Guianas at various scale levels: a synthesis. *Marine Geology*, 208, 141–151.
11 538 <https://doi.org/10.1016/j.margeo.2004.04.007>.
- 12 539 Bomer, E.J., Wilson, C.A., Hale, R.P., Hossain, A.N.M., Rahman, F.M.A., 2020. Surface elevation
13 540 and sedimentation dynamics in the Ganges-Brahmaputra tidal delta plain, Bangladesh:
14 541 Evidence for mangrove adaptation to human-induced tidal amplification. *Catena*, 187,
15 542 104312. <https://doi.org/10.1016/j.catena.2019.104312>
- 16 543 Boyd, R., Dalrymple, R.W., Zaitlin, B.A., 1992. Classification of clastic coastal depositional
17 544 environments. *Sedimentary Geology*, 80, 139-150. [https://doi.org/10.1016/0037-](https://doi.org/10.1016/0037-0738(92)90037-R)
18 545 0738(92)90037-R
- 19 546 Brunier, G., Tamura, T., Anthony, E. J., Gardel, A., Dussouillez, P., Todisco, D., van den Bel, M.,
20 547 2019. OSL chronology of sandy cheniers in French Guiana,” in: 1st Conference on Latin
21 548 American Physics of Estuaries and Coastal Oceans – LAPECO, Florianopolis.
- 22 549 Bureau de Recherches Géologiques et Minières, 2017. Etude de l'évolution
23 550 morphodynamique à l'embouchure du Maroni (MORPHOMAR) - Phase I. Rapport final.
24 551 BRGM/RP-66796-FR, Cayenne, French Guiana.
- 25 552 Bureau de Recherches Géologiques et Minières, 2019. Campagne d'acquisition sur l'évolution
26 553 morphodynamique à l'embouchure du Maroni (MORPHOMAR 17) - Phase II. Rapport final.
27 554 BRGM/RP-68442-FR, Cayenne, French Guiana.
- 28 555 Dalrymple, R.W., Choi, K., 2007. Morphologic and facies trends through the fluvial–marine
29 556 transition in tide-dominated depositional systems: A schematic framework for
30 557 environmental and sequence-stratigraphic interpretation. *Earth-Science Reviews* 81, 135-
31 558 174. DOI: 10.1016/j.earscirev.2006.10.002
- 32 559 Do, A.T.K., Huybrechts, N., Sottolichio, A., Gardel, A., 2019. Modeling and quantification of
33 560 patterns of salinity, mixing and subtidal flow in the Maroni estuary. *Proceedings of the 10th*
34 561 *International Conference on Asian and Pacific Coasts (APAC 2019) Hanoi.* 657–664.
35 562 https://doi.org/10.1007/978-981-15-0291-0_90
- 36 563 Do, A.T.K., Sottolichio, A., Huybrechts, N., Gardel, A. Circulation pattern and implication for
37 564 fine sediment transport in a preserved tropical estuary: the case of the Maroni (French
38 565 Guiana). Submitted, *Regional Studies in Marine Science*, this volume.
- 39 566 Dyer, K.R., 1997. *Estuaries: A Physical Introduction*. John Wiley & Sons, Chichester, 195 pp.
- 40 567 Gallay, M., Martinez, J.M., Mora, A., Allo, S., Mora A., Cochonneau G., Gardel, A., Doudou, J.C.,
41 568 Sarrazin, M., Chow-Toun, F., Laraque, A., 2018. Impact of land degradation from mining
42 569 activities on the sediment fluxes in two large rivers of French Guiana. *Land Degradation &*
43 570 *Development*, 29, 4323–4336. <https://doi.org/10.1002/ldr.3150>
- 44 571 Gardel, A., Anthony, E.J., Huybrechts, N., Lesourd, S., Santos, V., Sottolichio, A., 2019. River
45 572 estuaries of the Amazon-influenced Guianas coast: diversity and preliminary classification.
46 573 *Geophysical Research Abstracts*, Vol. 21, EGU2019-7414. EGU General Assembly 2019.

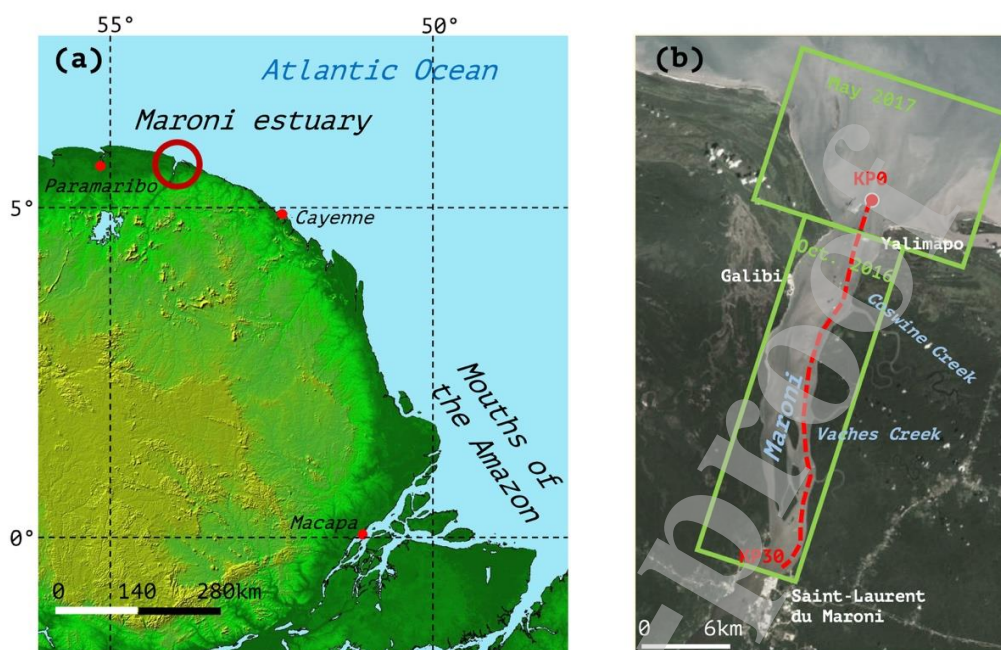
- 574 Geyer, W.R., Hill, P.S., Kineke, G.C., 2004. The transport, transformation and dispersal of
1 575 sediment by buoyant coastal flows. *Continental Shelf Research*, 24, 927-949.
2 576 DOI: 10.1016/j.csr.2004.02.006
- 3 577 Gratiot, N., Gardel, A., Anthony, E.J., 2007. Trade-wind waves and mud dynamics on the
4 578 French Guiana coast, South America: Input from ERA-40 wave data and field investigations.
5 579 *Mar. Geol.* 236, 15–26. <https://doi.org/10.1016/j.margeo.2006.09.013>
- 6 580 Grua, B., Cautru, J.P., 1993. Lithologie des Formations Superficielles: Mana-Saint-Laurent.
7 581 Unpublished BRGM Report. BRGM, Orléans, France.
- 8 582 Hein, C.J., Fitzgerald, D.M., de Souza, L.H.P., Georgious, J.Y., Buynevich, I.V., Klein, A.D.F., De
9 583 Menezes, J.T., Cleary, W.J., Scolaro, T.L., 2016. Complex coastal change in response to
10 584 autogenic basin infilling: An example from a sub-tropical Holocene strandplain.
11 585 *Sedimentology*, 63, 1362-1395.
- 12 586 Hori, K., Saito, Y., Zhao, Q., Cheng, X., Wang, P., Sato, Y. and Li, C., 2001. Sedimentary facies
13 587 and Holocene progradation rates of the Changjiang (Yangtze) delta, China.
14 588 *Geomorphology*, 41, 233-248.
- 15 589 Jolivet, M., Anthony, E.J., Gardel, A., Brunier, G., 2019a. Multi-decadal to short-term beach
16 590 and shoreline mobility in a complex river-mouth environment affected by mud from the
17 591 Amazon. *Front. Earth Sci.* 7, 1–17. <https://doi.org/10.3389/feart.2019.00187>
- 18 592 Jolivet, M., Gardel, A., Anthony, E.J., 2019b. Multi-decadal changes on the mud-dominated
19 593 coast of western French Guiana: implications for mesoscale shoreline mobility, river-mouth
20 594 deflection, and sediment sorting. *Journal of Coastal Research Special Issue* 88, 185-194.
21 595 DOI: 10.2112/SI88-014.1
- 22 596 Jounneau, J.M., Pujos, M., 1988. Suspended matter and bottom deposits in the Maroni
23 597 estuarine system (French Guiana). *Netherlands Journal of Sea Research*, 22, 99-108.
24 598 [https://doi.org/10.1016/0077-7579\(88\)90014-2](https://doi.org/10.1016/0077-7579(88)90014-2).
- 25 599 McBride, R.A., Taylor, M.J., and Byrnes, M.R., 2007. Coastal morphodynamics and chenier-
26 600 plain evolution in southwestern Louisiana, USA: a geomorphic model. *Geomorphology*, 88,
27 601 367-342.
- 28 602 Milliman, J.D., Meade, R.H., 1983. World-wide delivery of river sediment to the oceans. *J. Geol.*
29 603 91, 1–21.
- 30 604 Oliveira, C.J.M. de, Clavier, J., 2000. Variations spatio-temporelles des matieres en suspension
31 605 dans l'estuaire du Sinnamary, Guyane française: influence du barrage hydroélectrique de
32 606 Petit Saut. *Rev. Bras. Oceanogr.* 48, 29–39. <https://doi.org/10.1590/s1413-77392000000100003>
- 33 607
- 34 608 Orseau, S., Abascal Zorilla, N., Huybrechts, N., Lesourd, S., Gardel, A., 2020. Decadal-scale
35 609 morphological evolution of a muddy open coast. *Marine Geology*, 420, 106048.
36 610 <https://doi.org/10.1016/j.margeo.2019.106048>
- 37 611 Orseau, S., Lesourd, S., Huybrechts, N., Gardel, A., 2017. Hydro-sedimentary processes of a
38 612 shallow tropical estuary under Amazon influence. *The Mahury Estuary, French Guiana.*
39 613 *Estuar. Coast. Shelf Sci.* 189, 252–266. <https://doi.org/10.1016/j.ecss.2017.01.011>
- 40 614 Otvos, E. G., Price, W. A., 1979. Problems of chenier genesis and terminology: an overview.
41 615 *Mar. Geol.* 31, 251–263. doi: 10.1016/0025-3227(79)90036-7.
- 42 616 Plaziat, J.C., Augustinus, P.G.E.F. 2004. Evolution of progradation/erosion along the French
43 617 Guiana mangrove coast: a comparison of mapped shorelines since the 18th century with
44 618 Holocene data. *Mar. Geol.*, 208, 127–143. <https://doi.org/10.1016/j.margeo.2004.04.006>
- 45 619 Ross, L., Sottolichio, A., Maury, T., Lesourd, S., Gardel, A., 2019. Intratidal and subtidal
46 620 circulation in a tropical estuary during wet season : The Maroni, French Guiana.

621 <https://doi.org/10.3390/jmse7120433>

- 1 622 Rousseau, T.C.C., Roddaz, M., Moquet, J.S., Handt Delgado, H., Calves, G., Bayon, G., 2019.
2 623 Controls on the geochemistry of suspended sediments from large tropical South American
3 624 rivers (Amazon, Orinoco and Maroni). *Chem. Geol.* 522, 38–54.
4 625 <https://doi.org/10.1016/j.chemgeo.2019.05.027>
- 5 626 Saito, Y., Wei, H., Zhou, Y., Nishimura, A., Sato, Y. and Yokota, S., 2000. Delta progradation and
6 627 chenier formation in the Huanghe (Yellow River) delta, China. *Journal of Asian Earth
7 628 Science*, 18, 489– 497.
- 8 629 Tamura, T., Saito, Y., Nguyen, V. L., Ta, T. O., Bateman, M. D., Matsumoto, D., Yamashita, S.
9 630 (2012). Origin and evolution of interdistributary delta plains; insights from Mekong River
10 631 delta. *Geology*, 40, 303-306.
- 11 632 Savenije, H. H. G., 1989. Salt intrusion model for high-water slack, low-water slack and mean
12 633 tide on spreadsheet, *J. Hydrol.*, 107, 9–18. [https://doi.org/10.1016/0022-1694\(89\)90046-2](https://doi.org/10.1016/0022-1694(89)90046-2).
- 13 634 Shimozono, T., Tajima, Y., Akamatsu, S., Matsuba, Y., Kawasaki, A., 2019. Large-scale channel
14 635 migration in the Sittang River Estuary. *Scientific Reports*, 9: 9862.
15 636 <https://doi.org/10.1038/s41598-019-46300-x>
- 16 637 Sondag, F., Guyot, J.L., Moquet, J.S., Laraque, A., Adele, G., Cochonneau, G., Doudou, J.C.,
17 638 Lagane, C., Vauchel, P., 2010. Suspended sediment and dissolved load budgets of two
18 639 Amazonian rivers from the Guiana Shield: Maroni River at Langa Tabiki and Oyapock River
19 640 at Saut Maripa (French Guiana). *Hydrol. Process.* 24, 1433–1445.
20 641 <https://doi.org/10.1002/hyp.7603>
- 21 642 Sottolichio, A., Gardel, A., Huybrechts, N., Maury, T., Morvan, S., Lesourd, S., 2018. Premières
22 643 observations de la dynamique hydro-sédimentaire de l'estuaire Maroni (Guyane). *XV
23 644 Journées Natl. Génie Côtier - Génie Civ. La Rochelle*, 293–300.
24 645 <https://doi.org/10.5150/jngcgc.2018.033>
- 25 646 Todd, T., 1968. Dynamic Diversion: Influence of Longshore Current-Tidal Flow Interaction on
26 647 Chenier and Barrier Island Plains. *SEPM J. Sediment. Res. Vol. 38*, 734–746.
27 648 <https://doi.org/10.1306/74d71a5a-2b21-11d7-8648000102c1865d>
- 28 649 Uncles, R.J., 2002. Estuarine physical processes research: some recent studies and progress.
29 650 *Estuarine, Coastal and Shelf Science* 55, 829–856.
- 30 651 van Maren, D.S., 2005. Barrier formation on an actively prograding delta system: The Red River
31 652 Delta, Vietnam. *Marine Geology*, 224, 123-143.
- 32 653 Wolanski, E., 2007. *Estuarine Ecohydrology*. Elsevier, 157 pp.
- 33 654 Wong, Th. E., De Kramer, R., De Boer, P.L., Langereis, C., Sew-A-Tion, J., 2009. The influence of
34 655 sea level changes on tropical coastal wetlands: The Pleistocene Coropina formation,
35 656 Suriname. *Sediment. Geol.* 216, 127–137. Doi: 10.1016/j.sedgeo.2009.02.003
- 36 657 Wright, L.D., 1989. Dispersal and deposition of river sediments in coastal seas: Models from
37 658 Asia and the tropics. *Netherlands Journal of Sea Research*, 23, 493-500.
38 659 [https://doi.org/10.1016/0077-7579\(89\)90032-X](https://doi.org/10.1016/0077-7579(89)90032-X).

660 Figure Captions

669

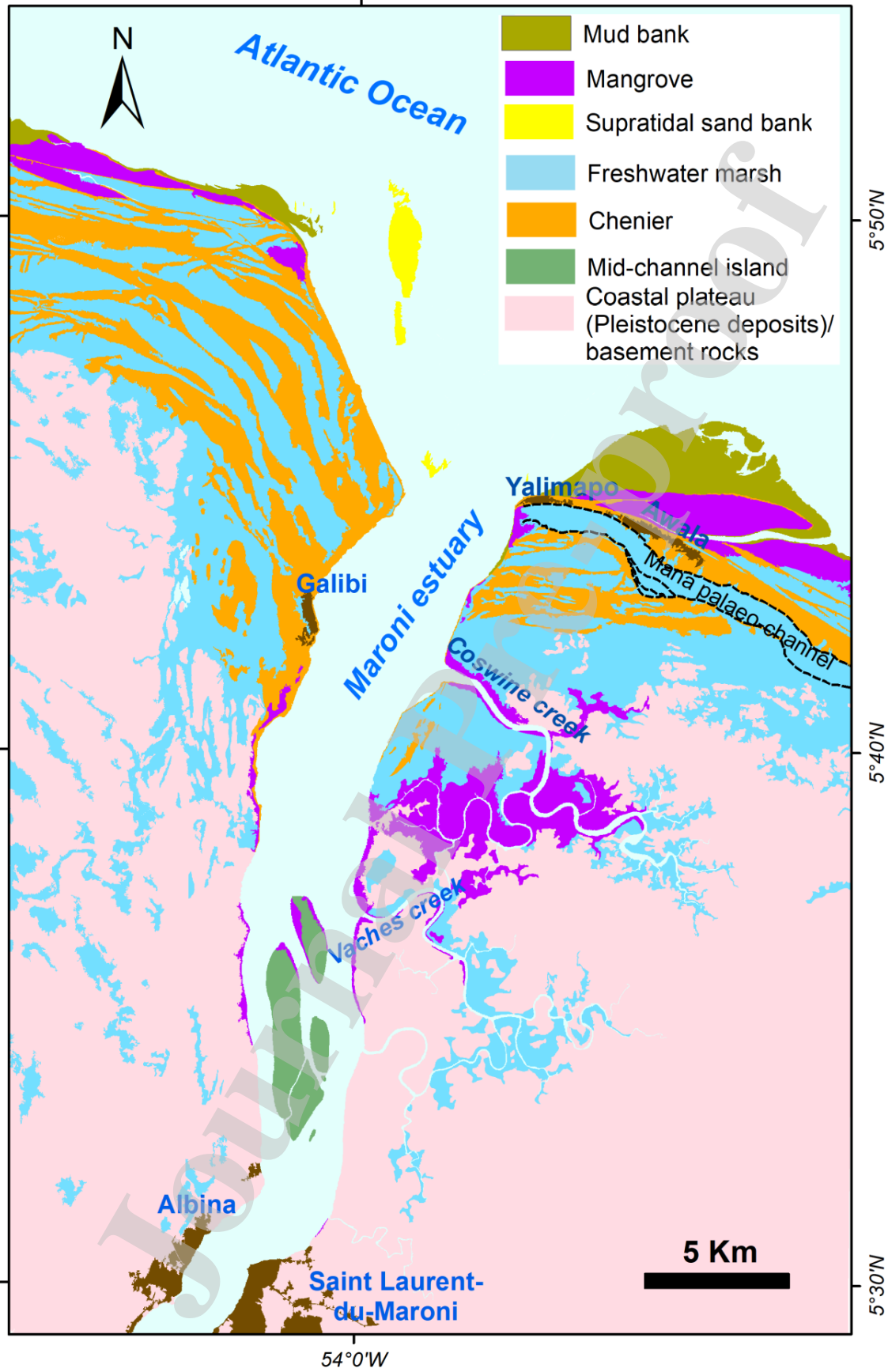


670

671

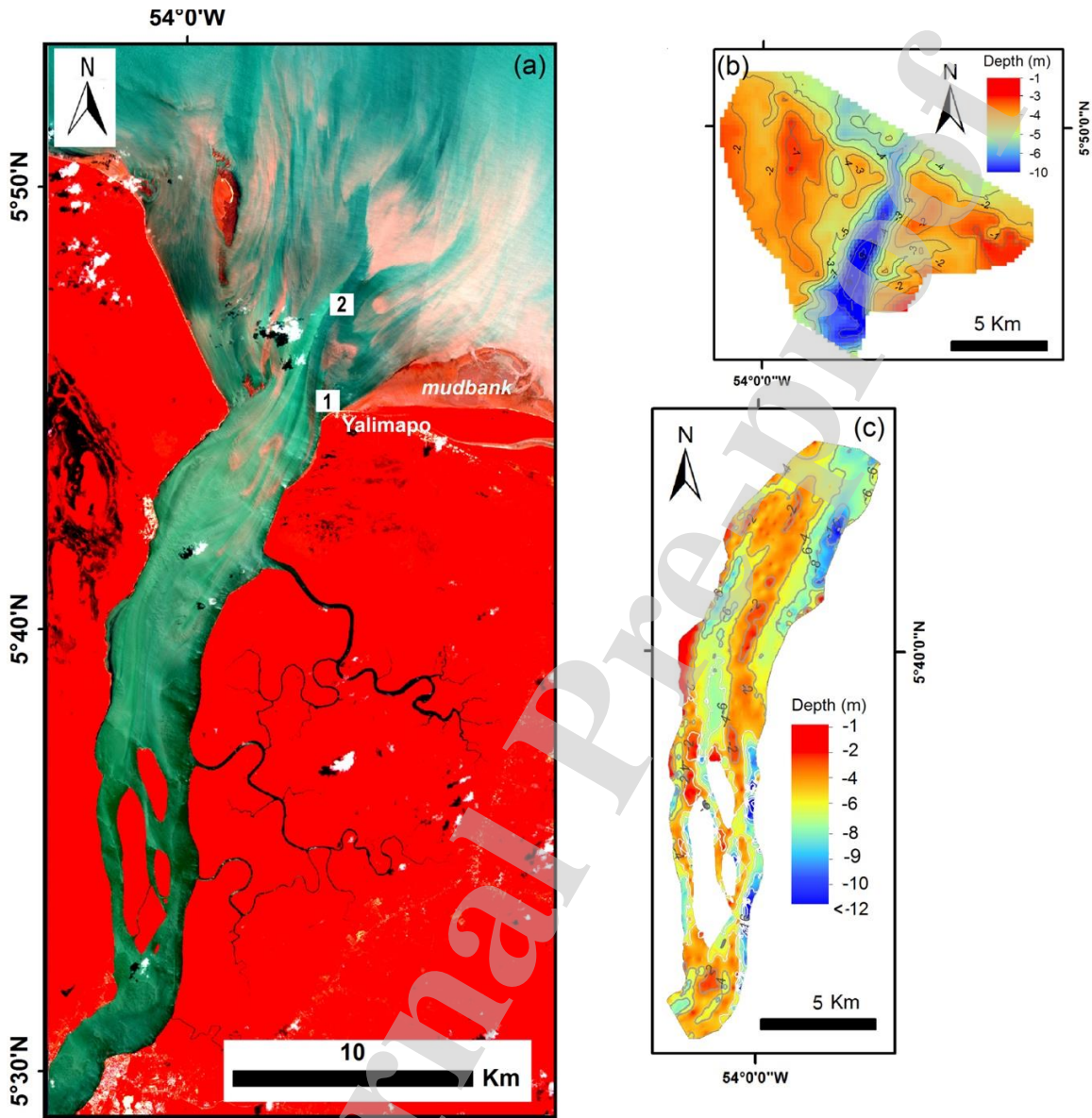
672 Figure 1. Regional setting of the Maroni River, South America, ~750 km northwest of the
 673 mouths of the Amazon (a), and the estuarine reach of the Maroni from kilometric point (KP)
 674 0 at the mouth to St. Laurent du Maroni at KP 30 (b), with broken red line showing transect
 675 along which the September 2019 salt and suspended sediment concentrations were
 676 measured, and area encased in green corresponding to two separate bathymetric surveys
 677 (October, 2016 and May, 2017).

678

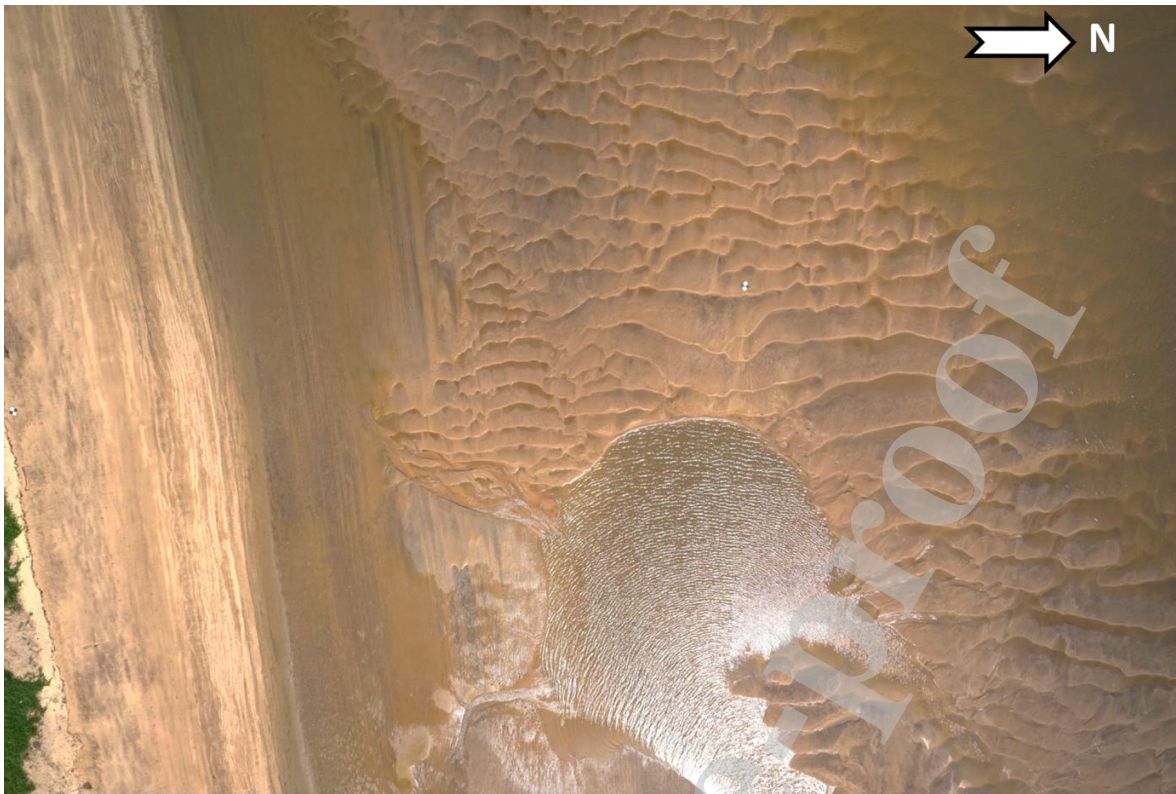


679

680 Figure 2. Map of morphological units of the Maroni River estuary and adjacent coast. The
 681 undifferentiated Pleistocene and basement units have been identified following Grua and
 682 Cautru (1993), and Augustinus, 2004).



683
 684 Figure 3. Sentinel 2B satellite image showing the mouth of the Maroni (a), bathymetry of the
 685 large estuary-mouth sand platform (May 2017 survey, b), and of the estuarine reach up to KP
 686 30 (October 2016 survey, c). 1 and 2 show locations of bedforms shown in Figs. 4 and 5.



687

688 Figure 4. Photo of 2D to 3D dunes exposed at low tide on the inner shoreface adjacent to the
689 beach at Yalimapo (see 1 in Fig. 3). These dunes migrate eastward under the influence of ebb-
690 dominant residual flow.

691

692

693

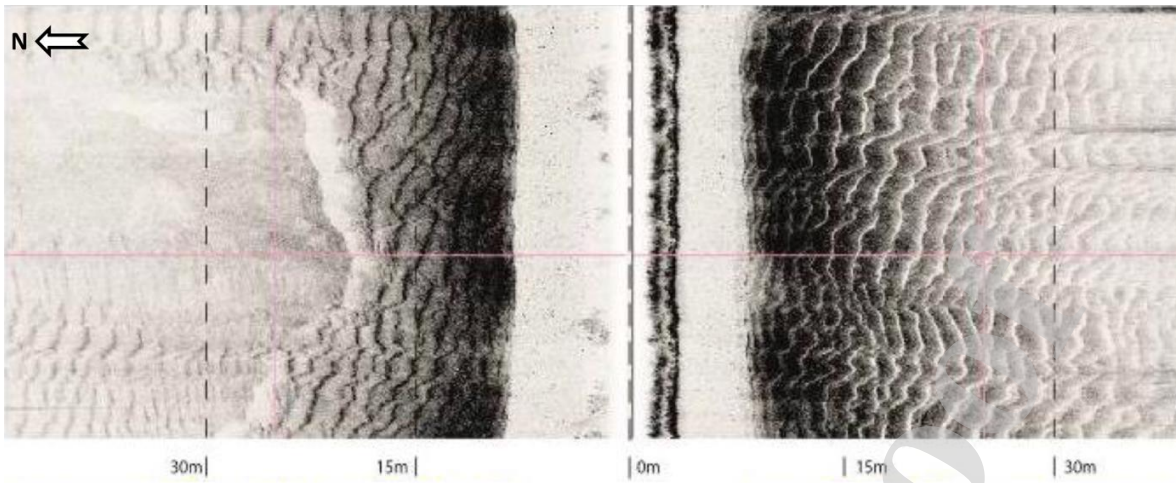
694

695

696

697

698



699

700 Figure 5. Side-scan sonar images of flood-dominant bedforms in the main Maroni channel (see
701 2 in Fig. 3; with kind permission from the Bureau de Recherches Géologiques et Minières,
702 2019).

703

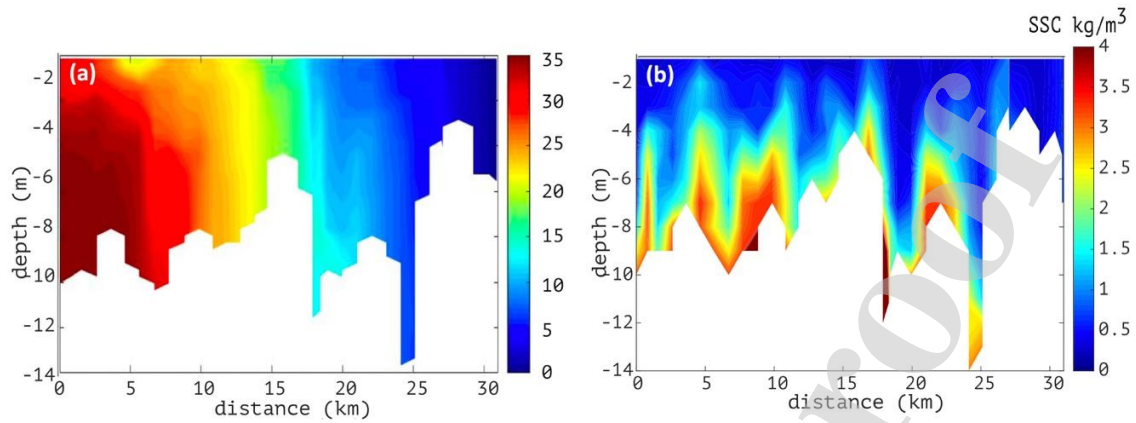
704

705

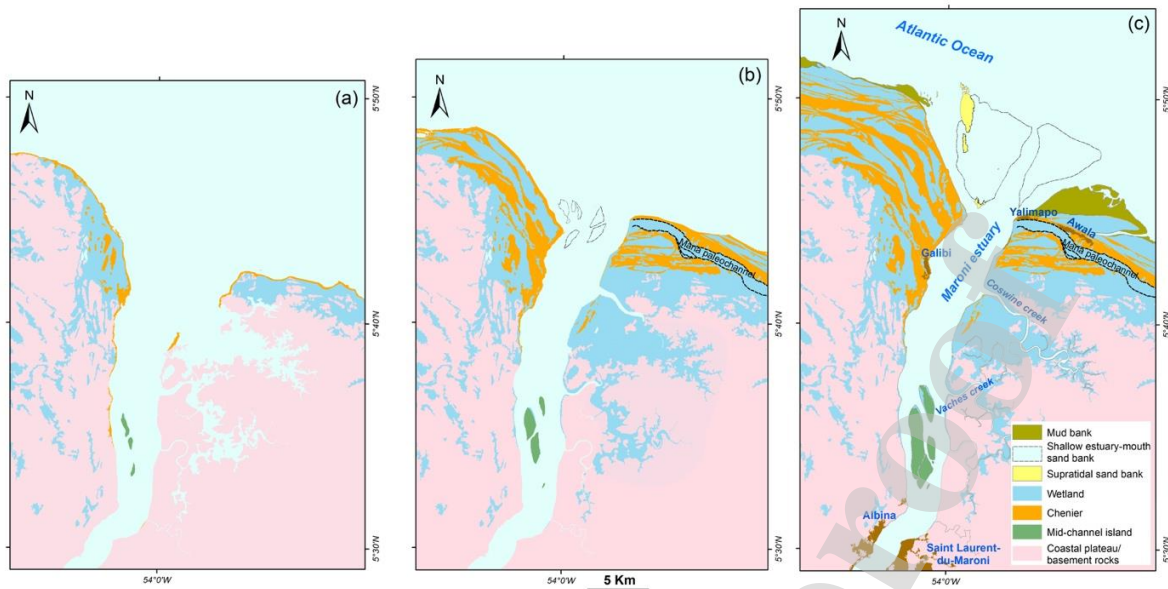
706

707

708



709
710 Figure 6. Salt (a) and suspended sediment concentrations in kg/m^3 (b) in the Maroni estuary
711 between KP 0 and KP 30 (see transect in Fig. 1b) measured on 29th September, 2019.



718

719 Figure 7. Simple schematic three-stage evolution of the Maroni estuary following the
 720 Holocene sea-level rise and still-stand: (a) young estuary flooded following the post-glacial rise
 721 in sea level and comprising bayhead cheniers; (b) median stage of estuarine development
 722 showing the increasing development of cheniers associated with the development of a coastal
 723 mud plain sourced by the distant Amazon, (c) present largely infilled estuarine stage and
 724 transition to delta associated with Maroni sand supply to the downdrift Suriname coast.

725

726

727

728

729

730

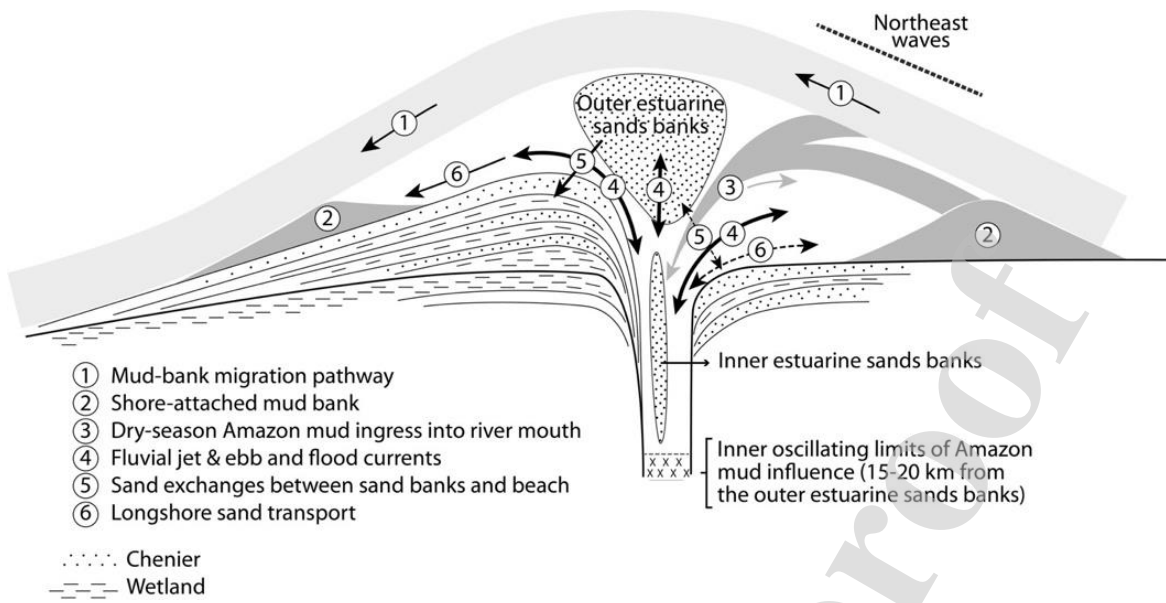


Figure 8. Sediment transport processes and pathways in the Maroni estuary.

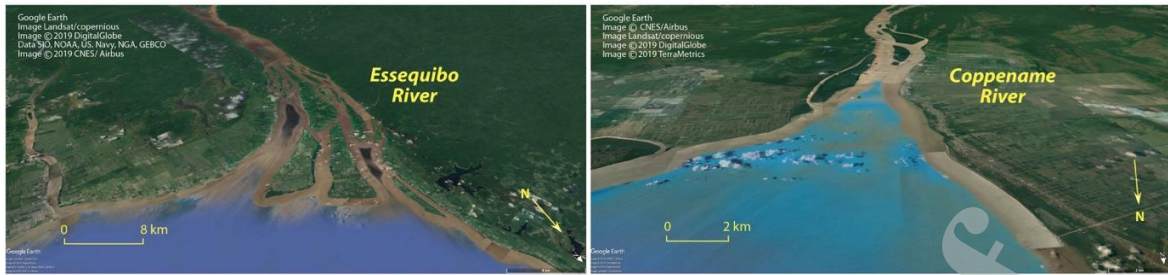


Figure 9. The mouths of the Essequibo River, Guyana (a), showing advanced infill and evolution towards a delta, and the Coppename River (b) where a large infilling estuary is still prevalent.

CRedit author statement

Antoine Gardel: Conceptualization, Methodology, Field work, Writing - Original draft preparation. **Edward Anthony:** Methodology, Field work, Writing - Original draft preparation, Reviewing and Editing. **Valdenira Ferreira dos Santos:** Field work, Visualization. **Nicolas Huybrechts:** Methodology, Validation. **Sandric Lesourd:** Methodology, Field work. **Aldo Sottolichio:** Methodology, Validation. **T. Maury:** Field work. **M. Jolivet:** Field work.

CRedit author statement

Antoine Gardel: Conceptualization, Methodology, Field work, Writing - Original draft preparation. **Edward Anthony:** Methodology, Field work, Writing - Original draft preparation, Reviewing and Editing. **Valdenira Ferreira dos Santos:** Field work, Visualization. **Nicolas Huybrechts:** Methodology, Validation. **Sandric Lesourd:** Methodology, Field work. **Aldo Sottolichio:** Methodology, Validation. **M. Jolivet:** Field work. **T. Maury:** Field work.

Conflict of interest

We declare no conflict of interest.

Journal Pre-proof